



OPEN ACCESS

EDITED BY

Lianliang Liu,
Ningbo University, China

REVIEWED BY

Miaoyun Zhao,
University of Nebraska-Lincoln,
United States
Xiaofeng Ma,
University of Chinese Academy
of Sciences, China
Bijun Xie,
Huazhong Agricultural University,
China

*CORRESPONDENCE

Qiuping Chen
cqpopen@163.com

SPECIALTY SECTION

This article was submitted to
Nutrition and Food Science
Technology,
a section of the journal
Frontiers in Nutrition

RECEIVED 13 July 2022

ACCEPTED 23 August 2022

PUBLISHED 08 September 2022

CITATION

Zhao N, Kong H, Liu H, Shi Q, Qi X and
Chen Q (2022) A network
pharmacology approach to evaluate
the synergistic effect
of dihydromyricetin and myricitrin
in vine tea on the proliferation
of B16F10 cells.
Front. Nutr. 9:993133.
doi: 10.3389/fnut.2022.993133

COPYRIGHT

© 2022 Zhao, Kong, Liu, Shi, Qi and
Chen. This is an open-access article
distributed under the terms of the
[Creative Commons Attribution License
\(CC BY\)](https://creativecommons.org/licenses/by/4.0/). The use, distribution or
reproduction in other forums is
permitted, provided the original
author(s) and the copyright owner(s)
are credited and that the original
publication in this journal is cited, in
accordance with accepted academic
practice. No use, distribution or
reproduction is permitted which does
not comply with these terms.

A network pharmacology approach to evaluate the synergistic effect of dihydromyricetin and myricitrin in vine tea on the proliferation of B16F10 cells

Nanxing Zhao, Hongming Kong, Hesheng Liu, Qing Shi,
Xiangyang Qi and Qiuping Chen*

College of Biological and Environmental Sciences, Zhejiang Wanli University, Ningbo, China

Aim of the study: Although vine tea has demonstrated broad-spectrum anti-cancer properties, its main active compounds, dihydromyricetin (DMY) and myricitrin (MYT), exert weaker effects than the tea extracts. This study aimed to investigate the synergistic inhibitory effects of DMY and MYT on B16F10 cell proliferation and their synergistic inhibitory effects.

Methods: The effect of vine tea extracts (VTEs) and their active compounds on B16F10 cells was analyzed by 3-(4,5-dimethylthiazol-2-yl)-2,5-diphenyltetrazolium bromide (MTT) assay, fluorescence staining, and flow cytometry. The synergistic effects were calculated by the combination index (CI), and its mechanism was discussed by network pharmacology.

Results: Different VTEs varied in their inhibition of B16F10 cell growth, with IC_{50} values ranging from 4.45 to 12.95 $\mu\text{g}/\text{mL}$. Among these, Guangzhou Qingyuan (Level 2), appeared to have the most potent inhibitory effect. The IC_{50} value of mix-use of DMY and MYT was 19.94~64.4 μM , of which DMY:MYT = 8:1 had the minimum IC_{50} value of 19.94 μM . Combinations in the 1:1~8:1 range had stronger effects than the isolated active compound. When they were mixed at the ratio of 1:4~8:1, $CI < 1$, showing a synergistic effect. The combination of DMY and MYT also significantly inhibited the tyrosinase activity in B16F10 cells, consistent with its impact on cell proliferation. The eight potential targets were identified by network pharmacology regulating melanin metabolism, tyrosine metabolism, and melanogenesis signaling. According to the analysis of protein-protein interactions, *TP53*, *TNF*, and *TYR* might be critical targets for preventing and treating melanoma.

Conclusion: We found that DMY and MYT induced apoptosis of B16F10 cells, and their combined application had a significant synergistic effect. The present findings indicated that vine tea had a multi-pathway and multi-target impact on the prevention and treatment of melanoma.

KEYWORDS

vine tea, dihydromyricetin, myricitrin, proliferation inhibition, network pharmacology, synergistic effect, cell cycle

Introduction

Melanoma originates from melanocytes (1, 2). In addition to genetic and other endogenous risk factors, ultraviolet radiation is the most critical exogenous risk factor for melanoma (3). Early detection and surgical resection are the best choices to cure melanoma. At the same time, radiotherapy and chemotherapy are also commonly used treatments (4). However, surgical resection is limited and cannot effectively treat metastatic tumors. Radiotherapy and chemotherapy have drug toxicity and a high cost (5, 6). Therefore, it is important to prevent melanoma through lifestyle. Phytochemicals as supplements have attracted wide attention because of their low cost and toxicity. Many active ingredients have been reported with anti-cancer, anti-metastatic, and pro-apoptotic effects (7–10). Daphnetin inhibits α -MSH-induced melanogenesis *via* PKA and ERK signaling pathways in B16F10 cells and inhibits melanin synthesis in UVB-irradiated HaCaT conditioned medium (11). Paclitaxel in combination with a C-C chemokine receptor type 7 monoclonal antibody can both delay B16F10 cell growth and reduce lymphatic metastasis (12). Luteolin inhibits melanoma growth by regulating cell-cell interaction and oncogenic pathways (13). The purified extract of *Nymphaea hybrid* also has a specific inhibitory effect on melanogenesis in B16F10 cells (14).

Vine tea (*Ampelopsis grossedentata*) has more than 600 years of use in China, is widely distributed in the mountainous areas of southern China, and has been used as a new food resource in recent years. It has hypoglycemic (15), antioxidant (16, 17), antibacterial (18), and anti-inflammatory (19, 20) properties. Several bioactive components have been isolated from vine tea, such as DMY, MYT, and myricetin (21). As the most abundant flavonoid in vine tea, the content of DMY can reach as much as 30% in the leaves (15). Several studies have shown it to be anti-tumor in human lung adenocarcinoma cell lines (22), human glioma (23), and cholangiocarcinoma (24).

Natural products have gained popularity due to their low toxicity and low cost. However, due to their complex composition, the use of natural products is sometimes restricted. Network pharmacology can provide insight into natural products. In network pharmacology, multiple targets of a specific molecule are analyzed through network analysis,

emphasizing multi-way regulation of signaling pathways, which can help understand the mechanism of prevention and treatment (25).

The present study evaluated the synergistic effect of the main active components in vine tea, DMY, and MYT, on the proliferation of B16F10 cells. The network pharmacological model was used to explain the underlying mechanisms of vine tea in preventing and treating melanoma.

Materials and methods

Materials

B16F10 cells were purchased from Shanghai Institute of Biochemistry and Cell Biology, CAS; MYT standard (CAS: 17912-87-7; \geq 98%, purity), DMY standard (CAS: 27200-12-0; \geq 98%, purity), and MTT were purchased from Beijing Solarbio Science and Technology Co., Ltd.; Fetal bovine serum was purchased from Beijing TransGen Biotech Co., Ltd.; RPMI medium and trypsin were purchased from Hyclone from Thermo Fisher Scientific; Hoechst 33342 was purchased from Shanghai Beyotime Biotechnology Co., Ltd.; PI/Rnase staining solution was purchased from Beijing BD Biosciences Co., Ltd., other reagents were commercially available and analytically pure. Six vine tea varieties selected for use in the experiment are all commercially available: A, Wild vine tea in Enshi, Hubei; B, Hubei Enshi selenium-rich vine tea; C, Guangzhou Qingyuan (Level 1); D, Guangzhou Qingyuan (Level 2); E, Wild vine tea in Shiqian, Guizhou; F, Wild vine tea in Zhangjiajie, Hunan.

Extraction of vine tea

The preparation of vine tea extracts (VTEs) was as follows: 70% ethanol was added to dried vine tea (tea: solvent = 1:10), and the suspension was incubated in a water bath at 40°C for 30 min. Then, the extracts were filtered and concentrated in a rotary evaporator to eliminate the solvent. Finally, the concentrate was lyophilized and stored at 4°C.

High-performance liquid chromatography analysis of vine tea extracts from different regions

VTEs were detected using a high-performance liquid chromatography (HPLC) system (Waters, Shanghai, China) with a C₁₈ (5 μm, 4.6 × 250 mm) reverse-phase column, and the flow rate was 1.0 mL/min. The mobile phases were 0.1% acetic acid acetonitrile solution (A) and 0.1% acetic acid aqueous solution (B). Under the following gradient profile: 0–22 min 10–30% A, followed by washing and reconditioning the column (3 min). The detection wavelength was 254 nm (200–400 nm full-band scanning).

The standard curve equation of DMY was $y = 9656905.4141x + 39250.3632$, $r^2 = 0.9995$ (0.1677 ~ 0.8 mg/mL); and MYT was $y = 33785171.6504x + 446.4681$, $r^2 = 0.9998$ (0.0030 ~ 0.035 mg/mL). The VTEs were prepared at a 1 mg/mL concentration, the sample injection volume was 20 μL and repeated three times as parallels.

Cell culture

B16F10 cells were inoculated in RPIM-1640 medium containing 10% FBS at 37°C and cultured in an incubator with 5% CO₂ and saturated humidity (MCO-15AC, Sanyo, Japan), and the medium was changed every other day. When cells reached about 80% confluence, they were digested and subcultured with 0.25% trypsin and allowed to continue to develop (26).

The proliferation of B16F10 cells by MTT assay

B16F10 cell suspension was inoculated in a 96-well plate at 3,000 cells/well for 24 h. VTEs were dissolved in dimethyl sulfoxide (DMSO) to 100 mg/mL and diluted with a culture medium to 10–30 μg/mL. For the administration of DMY and MYT, the compounds were diluted in DMSO to 100 mM and then diluted with a culture medium to get the needed concentration. The final concentration of the DMSO was less than 0.5% in the medium.

To evaluate the synergistic effect of DMY and MYT, cells were treated with DMY, MYT, or mix-use. In the mixture, the compounds were present in ratios of 1:4, 1:2, 1:1, 2:1, 4:1, and 8:1. After treatment for 72 h, 10 μL of 5 mg/mL MTT was added to each well. The media containing MTT was removed after 4 h, and 100 μL DMSO was added to each well to dissolve the formazan crystals (27). The plate was shaken for 1 min, the absorbance at 490 nm was measured, the inhibition rate of the drug on cell growth was calculated, and the general equation for the dose-effect relationship was obtained according to the following formula. The combination index (CI) was

calculated after 72 h incubation, and the CI value represented the combined effect of two drugs; CI < 1 showed synergism, CI = 1 additive effects, and CI > 1 showed antagonism. The CI values of different intervals had strong and weak differences. CI value was calculated by the equation.

$$\log (fa/fu) = \log (D/D_m)^m = m \log(D) - m \log(D_m)$$

D: the dose of the drug

D_m: the median-effect amount is signifying the potency.

Fa: the fraction affected by the dose

fu: the fraction unaffected, fu = 1-fa

If b = m, a = -mlogD_m, Y = log (fa/fu), X = logD, Y = bX+a.

$$CI = \frac{(D)_1}{(D_X)_1} + \frac{(D)_2}{(D_X)_2}$$

In the above formula, (D)₁ and (D)₂ represent the combined inhibition rate X% of drug 1 and drug 2 in the experiment, and (D_X)₁ and (D_X)₂ represent their respective inhibition rates X% (28).

Cell fluorescence staining

B16F10 cells were inoculated in 24-well plates at 3 × 10⁴ cells/well. DMY, MYT, or mixed-use were applied the next day at a concentration of 75 μM. The cells were stained for 72 h. The original medium was aspirated and discarded, and the well was washed with PBS. Each was stained with 250 μL Hoechst 33342 solution. After 15 min, the dye solution was discarded. After washing 3 times with PBS, fluorescence photomicrographs were obtained by an inverted fluorescence microscope (IX73, Olympus, Japan) (29) and quantitatively analyzed using ImageJ software.

$$\text{Mean} = \text{IntDen}/\text{Area} \quad (30).$$

Mean: Mean gray value.

IntDen: Integrated Density.

Effects of dihydromyricetin and myricitrin on tyrosinase activity in B16F10 cells

B16F10 cells were inoculated into 96-wells at 3,000 cells/well. The cells were cultured for 24 h before administering the test compounds. DMY and MYT were in DMSO to 100 mM and diluted with a culture medium to a concentration gradient of 20–100 μM, either alone or in combination.

After B16F10 cells were treated for 72 h, 90 μL 1% TritonX-100 was added to each well, and then 10 μL 1.0 mg/mL L-DOPA was added. The absorbance at 490 nm was measured after 5 min of ultrasound and treatment at 30°C for 30 min. The enzyme activity was calculated using the following formula: tyrosinase activity = OD_{sample} / OD_{control} × 100% (31).

Determination of cell cycle

The digested B16F10 cells were inoculated into three 12-well plates as three parallel groups at 5×10^4 cells/well. After 24 h, the cells were adherent to the wall before treatment. 75 μ M DMY, MYT, or the combined compounds were added to each well, and then the cells were incubated for 24 h. The digested cells were collected and centrifuged at 1,000 rpm for 5 min; then, the supernatant was discarded. After washing the cells with PBS twice, 4°C 75% ethanol was added slowly, and the cells were kept in darkness at 4°C overnight. The cells were centrifuged at 1,000 rpm for 5 min before analysis, the supernatant was discarded, and the cells were washed with PBS to remove all ethanol and resuspended in 0.5 mL PI/Rnase staining solution, incubated in the dark at room temperature for 15 min, and then analyzed by flow cytometry (FACSVerser, BD, America) (32).

Network analysis of component-disease interactions

The genes of targets associated with “melanoma” disease names were collected through CTD,¹ and the genes of targets with “DMY” and “MYT” as chemical names were similarly searched. Target genes were screened for overlapping with DMY, MYT, and melanoma. Then, they were uploaded to Cytoscape 3.8.2 to generate a network map of component-gene-disease interactions, and the protein interaction diagrams, gene ontology (GO), and kyoto encyclopedia of genes and genomes (KEGG) pathway diagrams were obtained for further analysis.

Data analysis and processing

Calculusyn 2.0 software was used to calculate the CI of DMY and MYT for further analysis. The data were visualized using by Origin 9.0 and were statistically analyzed by SPSS. For statistical analysis, one-way ANOVA was used. Results are presented as means and error bars represent standard deviation (SD). $p < 0.05$ was considered statistically significant.

Results

High-performance liquid chromatography analysis of vine tea extracts

VTEs were analyzed by HPLC (Figure 1), and three peaks revealed the main components of vine tea were DMY, MYT, and myricetin. The range of DMY was 53.36 ~ 67.09%, of which the

wild vine tea in Zhangjiajie, Hunan province, was the highest, with a content of 67.09% (Figure 2).

Inhibitory effects of vine tea extracts on the proliferation of B16F10 cells

B16F10 cells were treated with 10 μ g/mL VTEs, and the inhibition rate of cell proliferation increased gradually within 48 h (Figure 3). Within 24 h, the inhibition rate of VTEs on B16F10 cells was 9.87 ~ 53.62%. The inhibition rate was 14.87 ~ 75.95% within 48 h; the results showed that vine tea had an inhibitory effect on B16F10 cells. Among these, sample D had the best inhibitory effect.

Correlation analysis

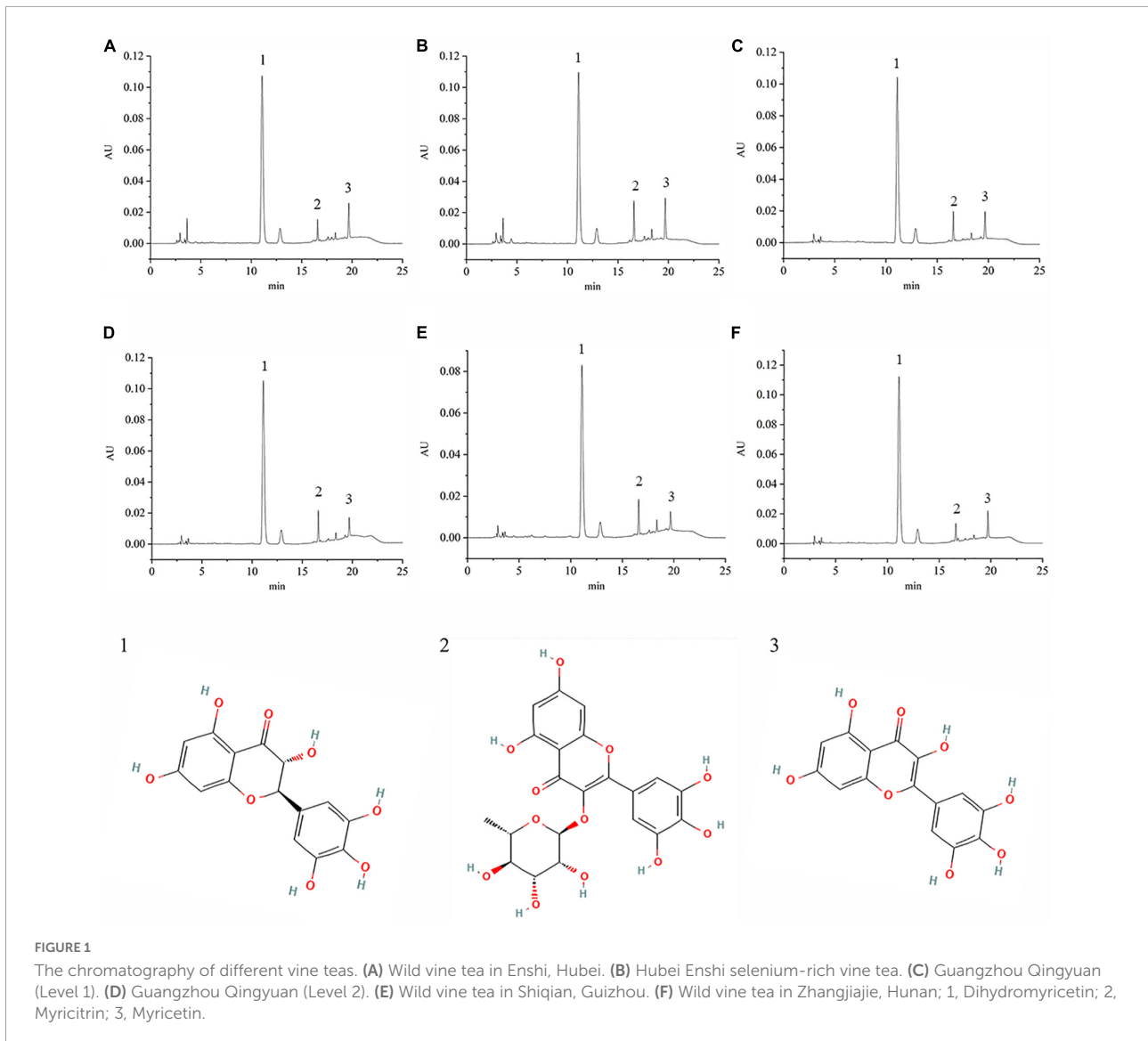
As shown in Table 1, Quantitative Composition-Activity Relationship analysis showed a very significant correlation between DMY and the proliferation inhibition rate of B16F10 cells, which indicated that DMY in vine tea played an essential role in inhibiting the proliferation of B16F10 cells.

Previous experiments showed that the IC₅₀ value of DMY on B16F10 cells was 14.73 μ g/mL. IC₅₀ of VTEs on B16F10 cells was 4.45~12.95 μ g/mL, in which sample D showed the best inhibitory effect (Figure 3). The IC₅₀ values of six VTEs were lower than DMY, indicating that VTEs had a better inhibitory effect on B16F10 cells. Therefore, we inferred that MYT in vine tea had no significant correlation with inhibiting B16F10 cell proliferation, but MYT may have a synergistic effect.

Inhibition of B16F10 cell proliferation by dihydromyricetin and myricitrin

Single or combined administration of DMY and MYT could inhibit the proliferation of B16F10 cells. The rate of cell proliferation inhibition increased gradually in a dose-dependent manner as drug concentration increased (Figure 4). When the content of DMY in the mixed drug increased, the IC₅₀ decreased gradually. When the DMY: MYT was more significant than 1: 1, the IC₅₀ of the mix-use group was lower than that of the single-drug group, and the lowest IC₅₀ was 19.94 μ M when DMY: MYT = 8:1 (Table 2). The CI value was used to analyze the experimental results further. DMY and MYT had a synergistic effect on inhibiting the proliferation of B16F10 cells. When they were mixed in the ratio of 1:4–8:1, the CI at IC₂₅, IC₅₀, and IC₇₅ was less than 1, showing a synergistic effect. Among them, the CI of IC₂₅ was the lowest, and DMY: MYT = 8:1 showed strong synergism, indicating that the synergistic effect of DMY and MYT was more apparent when the cell inhibition rate was low. Among different proportions, when the ratio of them was 8:1, the CI value was the lowest,

¹ <http://ctdbase.org/>



indicating that the synergistic effect of the ratio was the best (Figure 5).

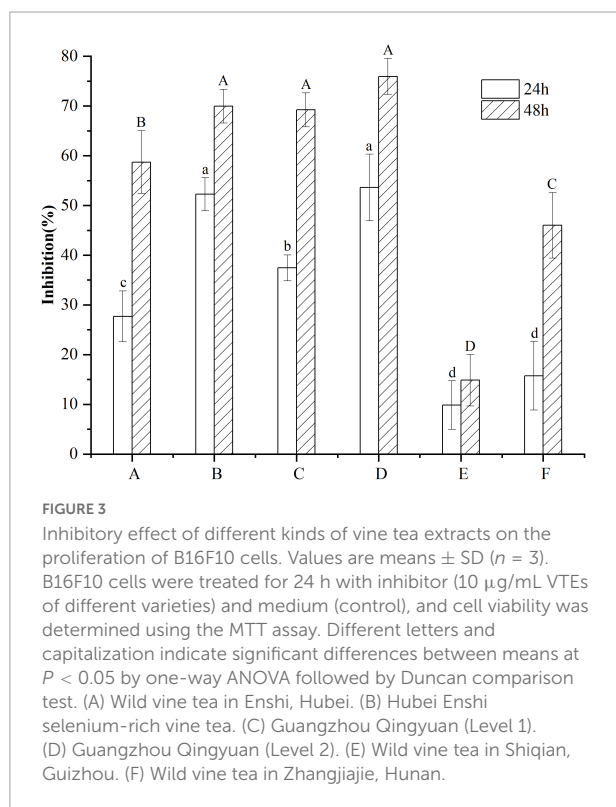
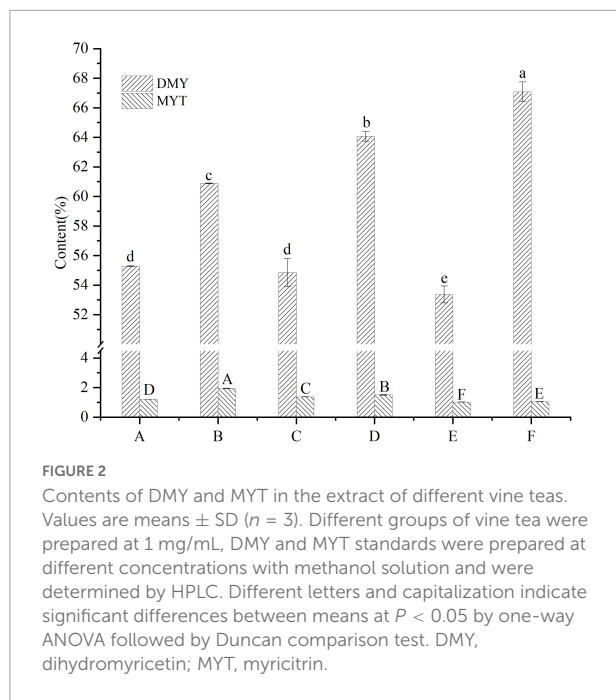
Effects of combination of dihydromyricetin and myricitrin on tyrosinase activity in B16F10 cells

DMY and MYT inhibited tyrosinase activity in B16F10 cells when applied alone or in combination. With the increase in drug concentration, the inhibition of tyrosinase activity increased gradually, showing a dose-dependent relationship in which the activity of DMY was more substantial than MYT's (Figure 6). The IC_{50} of the combined drug group was lower than that of the single-drug group. The lowest IC_{50} of DMY: MYT = 2:1 was

62.59 μ M (Table 3). When they were mixed in the ratio of 1:4–8:1, the CI of IC_{25} , IC_{50} , and IC_{75} was less than 1, showing a synergistic effect. Among them, the CI of IC_{75} was the smallest, and DMY: MYT = 8:1 showed strong synergism, indicating that the synergistic effect was higher when DMY and MYT were used together. Among the different ratio concentrations, the CI value of DMY: MYT = 8:1 was the lowest at IC_{50} and IC_{75} , while the lowest CI at IC_{25} was the ratio of 2:1 (Figure 7).

Inhibition of B16F10 cell proliferation by dihydromyricetin and myricitrin—Fluorescence staining

Hoechst's staining results showed that DMY and MYT alone or in combination could effectively inhibit the proliferation



of B16F10 cells and promote cell apoptosis compared with a control group. The fluorescent staining results were consistent with the MTT experimental data. With the increase of DMY concentration in the combined drug group, the number of cells decreased gradually, in which the single DMY was stronger than

TABLE 1 Correlation analysis.

Administration time	24 h		48 h	
	R	P	R	P
DMY	-0.882	<0.001	0.713	0.009
MYT	0.443	0.150	0.423	0.170
Myricetin	-0.562	0.057	0.540	0.070

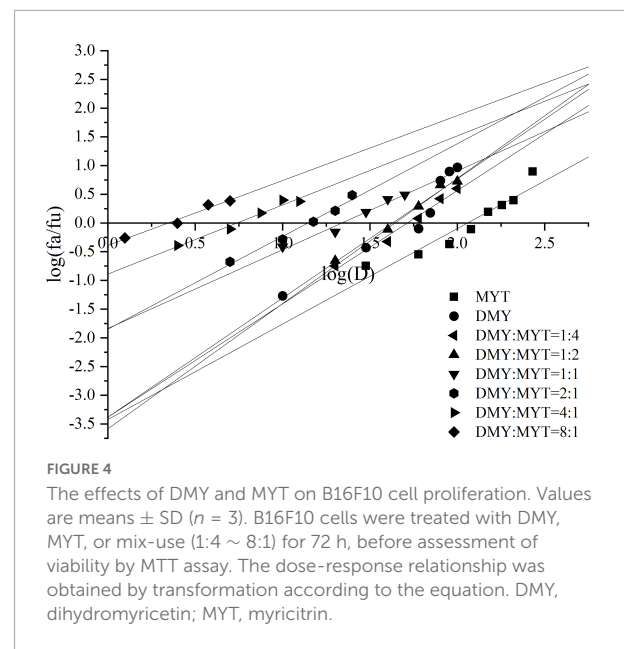


TABLE 2 Half-inhibitory concentration of drugs on B16F10 cell proliferation.

Sample	DMY	MYT	DMY: MYT					
			1:4	1:2	1:1	2:1	4:1	8:1
IC ₅₀ (μM)	45.98	109.1	64.64	63.89	43.65	41.87	27.41	19.94
r	0.9	0.95	0.99	0.99	0.99	0.99	0.98	0.98

MYT. The best effect was at 8:1 in the combined drug group (Figure 8A). The quantitative fluorescence results showed that the 8:1 group had the lowest mean fluorescence intensity, which was consistent with the image results (Figure 8B).

Effects of B16F10 cells on cell cycle in combination with dihydromyricetin and myricitrin

The effects of DMY and MTY on the cell cycle of B16F10 cells were analyzed by flow cytometry. As shown in Table 4, the results of DMY, MYT, and the combination group on the cell cycle of B16F10 cells were mainly characterized by reducing

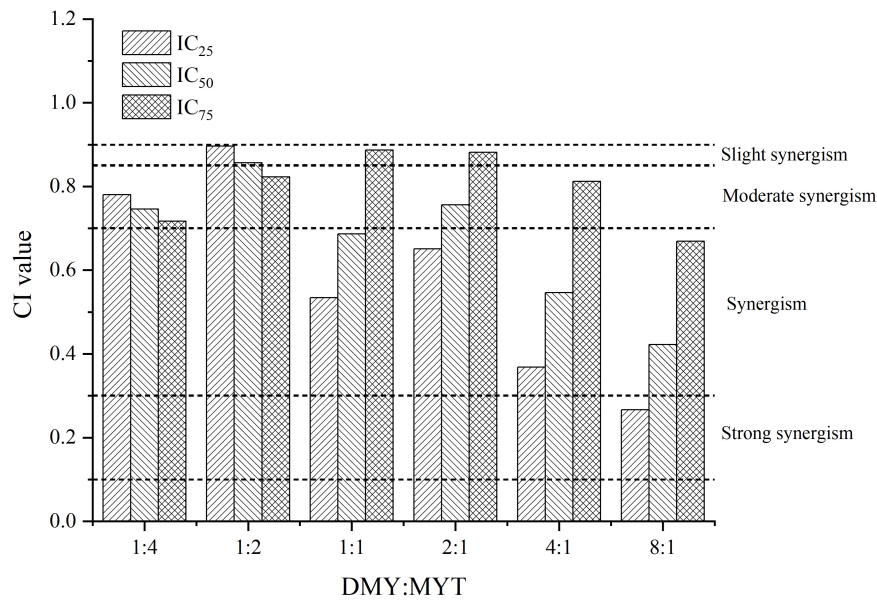


FIGURE 5 Analysis of the combined inhibitory effects of DMY and MYT on B16F10 cell proliferation. Values are means \pm SD ($n = 3$). B16F10 cells were treated with DMY, MYT, or mix-use (1:4 ~ 8:1) for 72 h, before assessment of viability by MTT assay. The CI value was calculated by the equation. DMY, dihydromyricetin; MYT, myricitrin.

the number of cells passing through G1 phase and blocking the cell cycle in S and G2 phases. The cell cycle results of the combination group (1:4, 1:2, 1:1, 2:1, 4:1, and 8:1) were similar to those of the DMY group, suggesting that their mechanisms of action were relatively consistent. Compared with the control

TABLE 3 Half-inhibitory concentrations of drugs on tyrosinase in B16F10 cells.

Sample	DMY	MYT	DMY: MYT					
			1:4	1:2	1:1	2:1	4:1	8:1
IC ₅₀ (μ M)	107.7	233.95	98.68	99.42	75.67	62.59	78.91	73.07
r	0.97	0.97	1	0.99	0.99	0.97	0.93	0.94

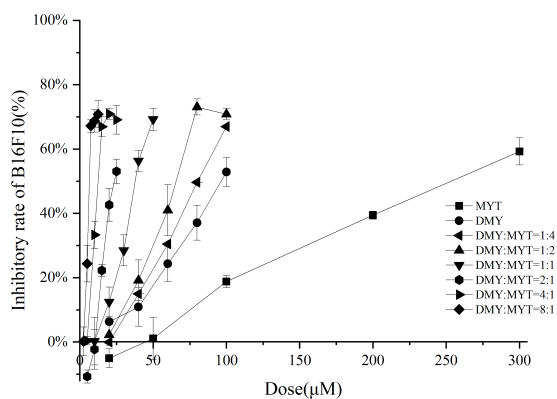


FIGURE 6 Tyrosinase inhibition by DMY and MYT in B16F10 cells. Values are means \pm SD ($n = 3$). After B16F10 cells were treated with DMY, MYT, or mix-use (1:4 ~ 8:1) for 72 h, 90 μ L of 1% TritonX-100 was added to each well, and then 10 μ L of 1.0 mg/mL L-DOPA was added. The absorbance at 490 nm was measured after 5 min of ultrasound and treatment at 30°C for 30 min. The dose-response relationship was obtained by transformation according to the equation. DMY, dihydromyricetin; MYT, myricitrin.

group, the experimental groups had significant differences, of which DMY: MYT = 8:1 group was the most prominent, and the percentage of cells in the G1 phase decreased to 59.38%, the rate of cells in the S phase increased to 33.16% and the cells in G2 phase increased to 7.46%.

Targets of dihydromyricetin and myricitrin on melanoma

The mechanism of action of vine tea in the prevention and treatment of melanoma was studied. The targets of DMY and MYT on melanoma were shown in **Figure 9A**. 8 targets of DMY and MYT related to melanoma, among which DMY acted on *TYRPI*, *PARP1*, *MC1R*, and *TYR*, while MYT acted on *TP53*, *TNF*, *PPARG*, and *PTGS2*.

Two components-disease cross targets were uploaded to the String database to construct a protein-protein interaction network (PPI). In this network, eight targets

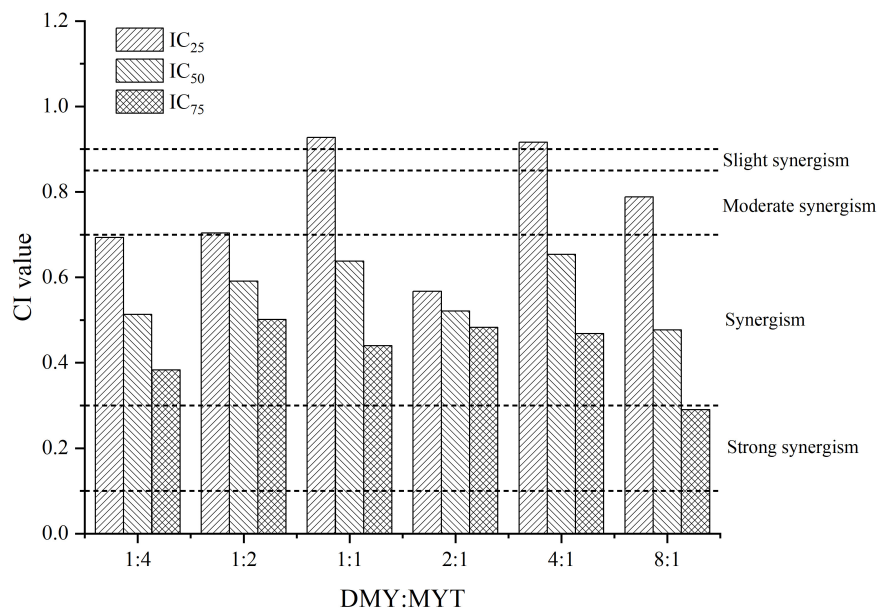


FIGURE 7

Analysis of the combined effect of DMY and MYT on inhibiting tyrosinase in B16F10 cells. Values are means \pm SD ($n = 3$). After B16F10 cells were treated with DMY, MYT, or mix-use (1:4 ~ 8:1) for 72 h, 90 μ L of 1% TritonX-100 was added to each well, and then 10 μ L of 1.0 mg/mL L-DOPA was added. The absorbance at 490 nm was measured after 5 min of ultrasound and treatment at 30°C for 30 min. The dose-response relationship was obtained by transformation according to the equation. The CI value was calculated by the equation. DMY, dihydromyricetin; MYT, myricitrin.

could interact with proteins, and 14 edges represent the interactions between proteins. The average degree of freedom of each node in the network was 3.5, the average betweenness centrality was 0.101190, and the average closeness centrality was 0.645117 (Figure 9B). There were three targets above the average, speculating that *TP53*, *TNF*, and *TYR* might be the critical targets of vine tea in preventing and treating melanoma (Table 5). Interleukin-4 and 13 signaling, thyroid cancer, pathways in cancer, signaling by interleukin, interleukin-10 signaling, melanogenesis, melanin biosynthesis, and tyrosine metabolism might be the key to treating melanoma.

GO pathway enrichment analysis

The functional enrichment analysis of GO terms was carried out. A total of 474 enrichment results were obtained in the biological process ($P < 0.01$), and 10 categories with the highest functional values were selected, mainly related to the metabolic synthesis of melanin, including the corresponding response to light stimulation and the negative regulation of gene silencing. Twenty six enrichment results were obtained by molecular function, mainly related to oxidoreductase activity, and 12 enrichment results were obtained by cell composition, including melanosome membrane, and complex transcription mechanism (Figure 10A).

KEGG pathway enrichment analysis

The selected targets were analyzed by KEGG pathway enrichment analysis, and 6 enrichment results were obtained ($P < 0.01$). It included the melanogenesis signaling pathway, NF- κ B signaling pathway, tyrosine metabolism signaling pathway, thyroid cancer signaling pathway, and apoptosis signaling pathway, suggesting that DMY and MYT play a role in preventing and treating melanoma by acting on the multiple pathways (Figure 10B).

Discussion

Melanoma is challenging to treat because of its ability to metastasize at early stages and its resistance to conventional cancer treatments (33, 34). The use of molecular targeted drugs and immunotherapy for melanoma is limited by the high cost and significant side effects (2). Therefore, safer and more effective treatments are necessary. Natural products have few side effects and do not contain any drug residues. The compatibility of active components can improve disease prevention and treatment efficacy and has been widely used in anti-tumor. For example, *Cuphea aequipetala* extracts can induce cell accumulation in the G1 phase of the cell cycle, induce apoptosis, and thus exhibit inhibitory activity (35). Menke et al. reported that dandelion extract and mistletoe

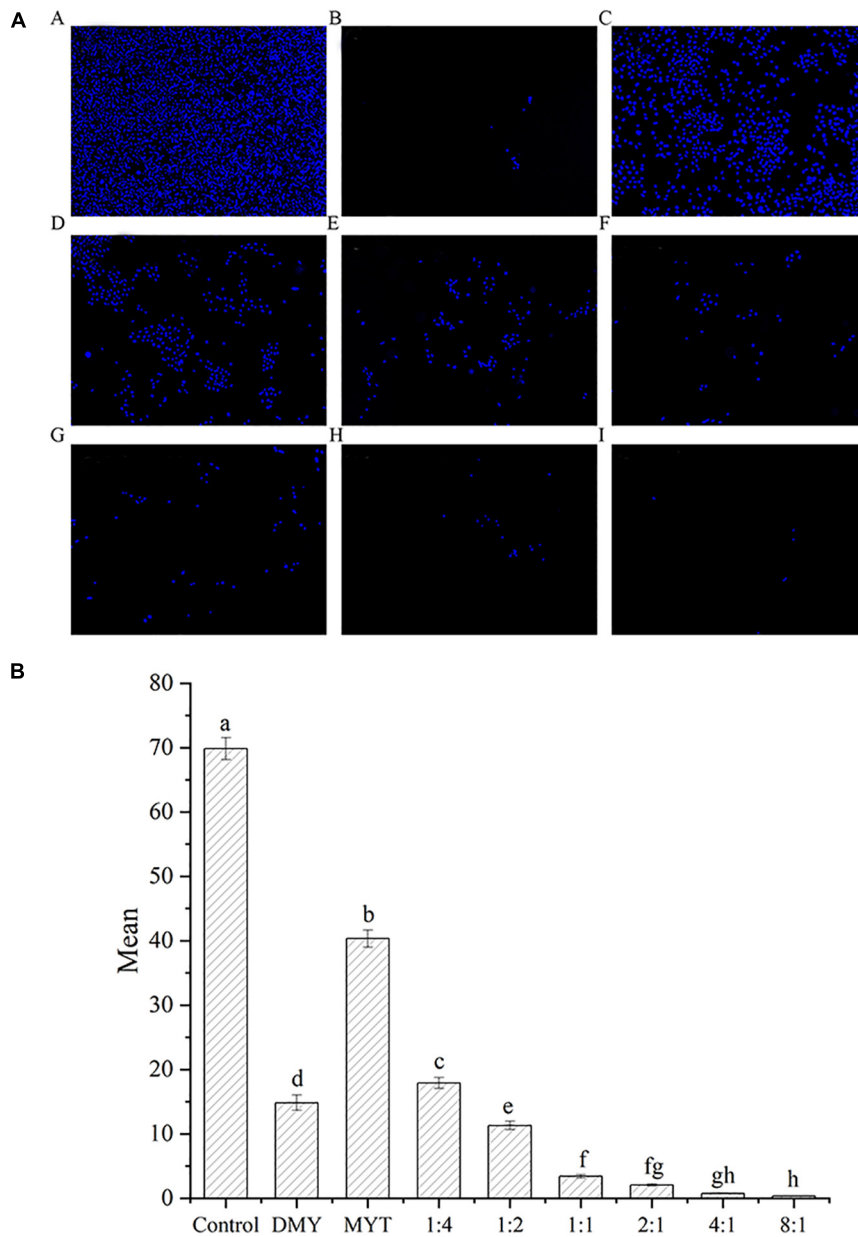


FIGURE 8 Analysis of the synergistic inhibitory effect of DMY and MYT on cell proliferation by fluorescence staining. Cell viability was determined by Hoechst 33342 fluorescent staining and pictures were quantified with ImageJ. Values are means \pm SD ($n = 3$). Different letters indicate significant differences between means at $P < 0.05$ by one-way ANOVA followed by Duncan comparison test. **(A)** Fluorescence photography. **(B)** Fluorescence quantitative analysis. (A) Control. (B) DMY. (C) MYT. (D) DMY: MYT = 1:4. (E) DMY: MYT = 1:2. (F) DMY: MYT = 1:1. (G) DMY: MYT = 2:1. (H) DMY: MYT = 4:1. (I) DMY: MYT = 8:1. DMY, dihydromyricetin; MYT, myricitrin; Mean, mean gray value.

extract could promote neuroblastoma cell apoptosis (36). Sturza et al. found that quercetin could simultaneously regulate the pathway of glycolysis and mitochondria to produce ATP to kill cancer cells (37). Some studies have shown that flavonoids can inhibit *mTOR* and *RAS* carcinogenic pathways, activate apoptosis, and lead to cell cycle stagnation. The vine tea contains many flavonoids, which have certain biological activities in cells and have anti-tumor effects (38). Huang et al. found

that DMY inhibits melanin synthesis through its antioxidant properties and down-regulation of protein kinase A, protein kinase C, and mitogen-activated protein kinase signal pathways (39). Our data showed that the VTEs could inhibit B16F10 cells, and the inhibitory effect on tyrosinase was consistent with cell inhibition experiments. In organisms, tyrosinase is the key enzyme involved in melanin biosynthesis (31). It has been reported that individual flavonoids are potential melanin

TABLE 4 Effects of the drugs on the cell cycle of B16F10 cells.

Sample	Control	DMY	MYT	DMY: MYT					
				1:4	1:2	1:1	2:1	4:1	8:1
G1/%	75.9 ± 0.58a	59.11 ± 2.00d	67.81 ± 5.3b	63.5 ± 0.75c	59.32 ± 0.05d	60.36 ± 1.39cd	62.17 ± 1.26cd	59.96 ± 0.45cd	59.38 ± 1.43cd
S/%	22.05 ± 1.39d	35.32 ± 1.10a	27.25 ± 4.97c	28.51 ± 0.75bc	35.73 ± 0.13a	33.56 ± 1.41ab	32.44 ± 1.53ab	34.79 ± 1.01a	33.16 ± 1.2ab
G2/%	2.05 ± 0.82d	5.57 ± 0.94bc	4.96 ± 0.33c	7.98 ± 0.03a	4.96 ± 0.17c	6.08 ± 0.39b	5.39 ± 0.29bc	5.26 ± 0.57bc	7.46 ± 0.23a

The mean value of different letters in the same row is significantly different from the mean value of control ($P < 0.05$).

synthesis inhibitors in mammalian melanocytes (40, 41). For melanoma diseases, only flavonoids with an IC_{50} value of less than 50 μ M can inhibit mammalian tyrosinase, thus reducing the melanin synthesis of B16F10 (31).

Some studies have shown that natural products target pathogens through a combination of different structures and functions (42). The active components in vine tea are present as mixtures. The activity of purified extracts of single compounds is weaker than that of crude extracts, suggesting that maximum bioactivity is obtained through the interaction of different functional factors (43). Previous studies have compared the theoretical value (T-EM) with the actual experimental value (EM). If the EM is higher than the T-EM, the two compounds are considered to have a synergistic effect. The EM value is the sum of the effect values of each combination. For example, it has been found that the synergistic effect of EGCG and metformin can increase ROS, thereby destroying the ribonucleic acid of B16F10 cells and promoting cell apoptosis (44). These flavonoids have also been shown to inhibit melanoma (37). This inhibitory effect has two main aspects: inhibiting cancer cell proliferation and promoting cancer cell apoptosis (45–47). Recent studies have shown inhibitory effects on the expansion of human acute promyelocytic leukemia cells and K562 cells (48), Bel-7402 cells (49), human breast cancer cells (50, 51), and nasopharyngeal carcinoma HK-1 cells (27). We expected that both DMY and MYT would have inhibitory effects on B16F10 cells. However, the IC_{50} value of DMY on B16F10 cells was 14.73 μ g/mL, the IC_{50} of MYT on B16F10 cells was 50.66 μ g/mL, and the IC_{50} of VTEs on B16F10 cells was 4.45–12.95 μ g/mL, which showed that the effect was not as significant as a crude extract. We hypothesized that the combination of active compounds in the extracts could enhance the inhibitory effect on melanoma disease. Therefore, the correlation between DMY, MYT, and myricetin in vine tea was analyzed, and DMY had a very significant correlation. Further inhibition experiments showed that the IC_{50} of VTEs was lower than that of DMY. There might be a synergistic effect between the active compounds. We selected DMY and MYT for further study since our previous experimental results indicated that DMY and myricetin had no synergistic effect, whereas DMY and MYT did show an effect. B16F10 cells were treated with different ratios of DMY and MYT, ranging from 1:4 to 8:1; it was found that DMY: MYT = 8:1

was the most effective in inhibiting B16F10 and tyrosinase activity. Fluorescence staining showed that the number of cells decreased with the increase of DMY concentration, and the inhibitory effect of DMY was more substantial than MYT's. Compared with the control group, the proportion of cells in S phase, or G2 phase was increased, but G1 phase was decreased. The effects of DMY and MYT on B16F10 cells were analyzed by flow cytometry, which showed that the cell cycle was arrested in the S phase and G2 phase. The combined treatment could effectively reduce the number of cells entering the G1 phase. The inhibition of DMY on melanoma cells was higher than that of MYT. We speculated that the proportion of DMY had an important effect on the synergism. It was observed that the IC_{50} values of the mix-drugs decreased with increased DMY content. Especially in the range of 1:1~8:1, they showed lower IC_{50} than single-use. Based on CI and isobole methods, the 8:1 group showed a strong synergistic effect. However, only a narrow range of ratios were tested in this experiment; perhaps increasing the ratios will produce stronger effects, which will be tested in the follow-up experiments.

Furthermore, network pharmacology was used to create a network map of the "active ingredient-acting gene-disease" of vine tea on melanoma disease. It was found that DMY and MYT have the same target and act on eight different targets of melanoma disease, which might be the reason for the synergism between DMY and MYT. Based on the interaction analysis of these targets, *TP53*, *TNF*, and *TYR* might be the key targets for the prevention and treatment of melanoma diseases. P53 protein promoted cancer cell apoptosis by responding to the anti-proliferation effects of various physiological processes such as aging (52). GO, and KEGG enrichment analysis found that the prevention and treatment of melanoma were related to ultraviolet reaction, melanosome membrane, chitosan, receptor binding, NF- κ B signal pathway, and apoptosis. Abnormal expression of NF- κ B has been associated with various cancers (53). Exposure to ultraviolet (UV) radiation, that is, UVA (315–400 nm), and UVB (280–315 nm), is considered to be a significant risk factor for melanoma (54). Melanosomes could synthesize and organize melanin. Melanin synthesis and melanosome transport disorders are associated with pigmented diseases (55). The crosstalk between protease-activated receptor 1 and platelet-activating factor receptor has been demonstrated

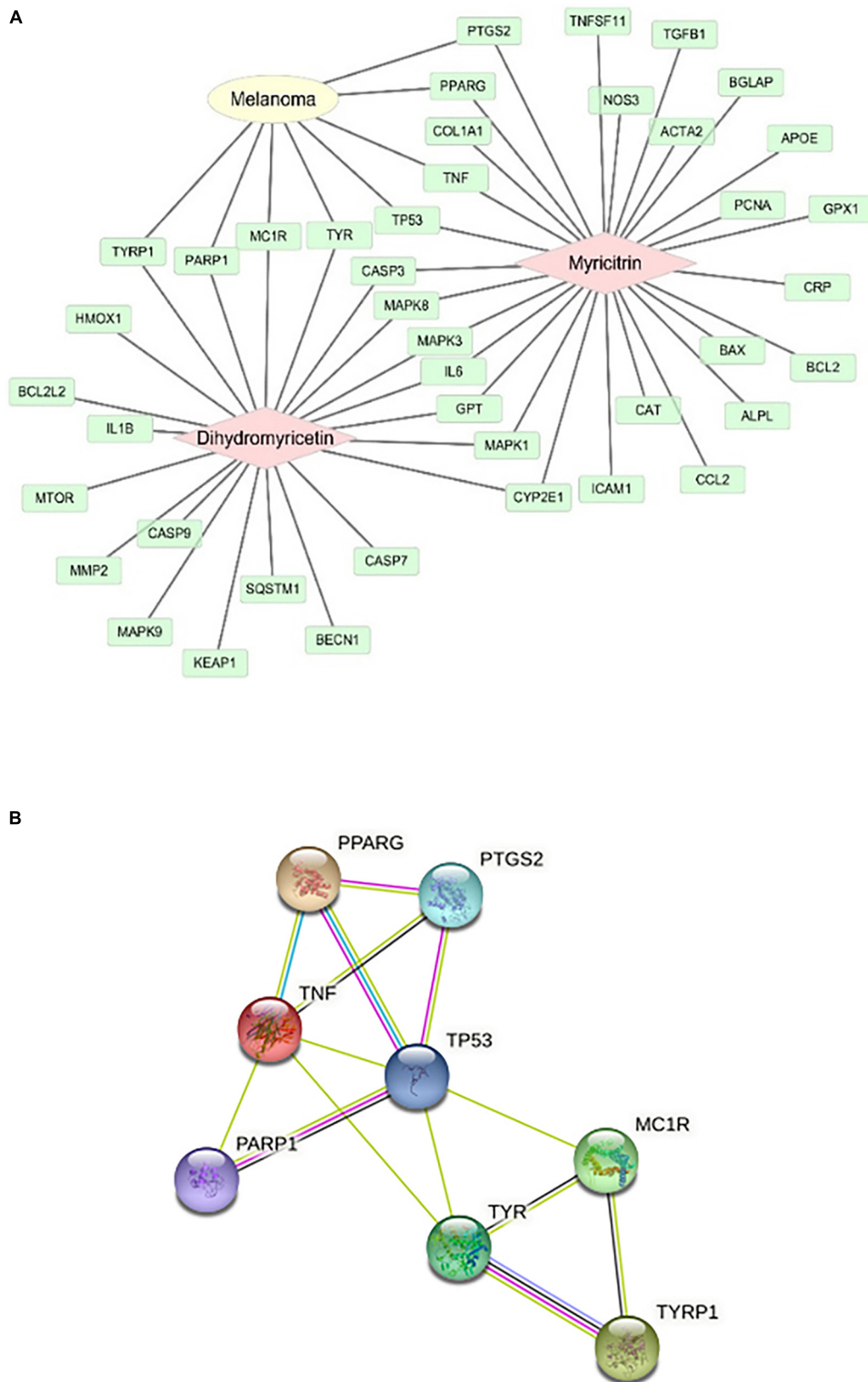


FIGURE 9
 Analysis of action targets of DMY and MYT on melanoma. **(A)** The targets of dihydromyricetin and myricitrin on melanoma. **(B)** The protein-protein interaction network of DMY, MYT, and melanoma disease.

TABLE 5 Basic information of crucial gene in the control of melanoma by vine tea.

Gene	Pathway	Degree	Betweenness	Closeness
TP53	Interleukin-4 and 13 signaling, thyroid cancer, pathways in cancer, signaling by Interleukins	6	0.381	0.875
TNF	Interleukin-4 and 13 signaling, signaling by interleukins, interleukin-10 signaling	5	0.167	0.778
TYR	Melanogenesis, melanin biosynthesis, tyrosine metabolism	4	0.190	0.700

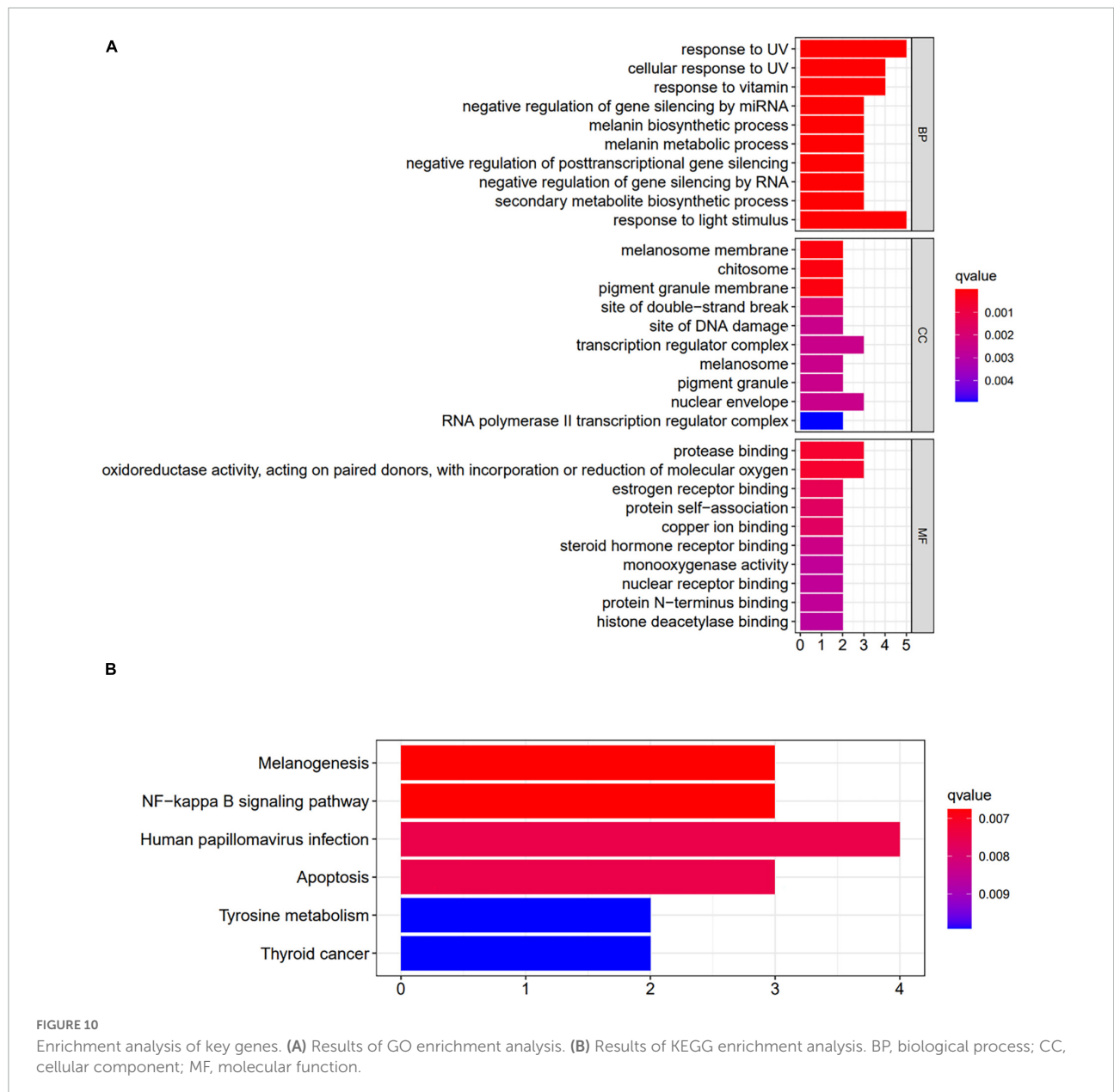


FIGURE 10

Enrichment analysis of key genes. (A) Results of GO enrichment analysis. (B) Results of KEGG enrichment analysis. BP, biological process; CC, cellular component; MF, molecular function.

to regulate the expression of melanoma cell adhesion molecule (MCAM/MUC18) metastasis of melanoma (56).

Conclusion

The combination of DMY and MYT in vine tea could synergistically inhibit the proliferation of B16F10 cells, and they have a synergistic effect on different targets. Through network pharmacology, it is concluded that *TP53*, *TNF*, and *TYR* are the main targets of DMY and MYT in melanoma disease and regulate signaling pathways such as melanogenesis, NF- κ B, and apoptosis. Regular application of low-toxicity and vine tea extract can contribute to the prevention and treatment of melanoma.

Data availability statement

The original contributions presented in this study are included in the article/supplementary material, further inquiries can be directed to the corresponding author/s.

Author contributions

QC and XQ designed the study. NZ and HK performed the experiments, sorted out the data, and drew the drawings. HL and QS provided the experimental guidance.

References

- Quintanilla-Dieck MJ, Bichakjian CK. Management of early-stage melanoma. *Facial Plast Surg Clin North Am.* (2019) 27:35–42. doi: 10.1016/j.fsc.2018.08.003
- Namikawa K, Yamazaki N. Targeted therapy and immunotherapy for melanoma in Japan. *Curr Treat Options Oncol.* (2019) 20:7. doi: 10.1007/s11864-019-0607-8
- Lodde G, Zimmer L, Livingstone E, Schadendorf D, Ugurel S. [Malignant Melanoma]. *Hautarzt.* (2020) 71:63–77. doi: 10.1007/s00105-019-04514-0
- Puza CJ, Bressler ES, Terando AM, Howard JH, Brown MC, Hanks B, et al. The emerging role of surgery for patients with advanced melanoma treated with immunotherapy. *J Surg Res.* (2019) 236:209–15. doi: 10.1016/j.jss.2018.11.045
- Austin E, Mamalis A, Ho D, Jagdeo J. Laser and light-based therapy for cutaneous and soft-tissue metastases of malignant melanoma: a systematic review. *Arch Dermatol Res.* (2017) 309:229–42. doi: 10.1007/s00403-017-1720-9
- Zhang Q, Jin L, Jin Q, Wei Q, Sun M, Yue Q, et al. Inhibitory effect of dihydroartemisinin on the proliferation and migration of melanoma cells and experimental lung metastasis from melanoma in mice. *Front Pharmacol.* (2021) 12:727275. doi: 10.3389/fphar.2021.727275
- Ghazizadeh F, Shafiei M, Falak R, Panahi M, Rakhshani N, Ebrahimi SA, et al. Xanthomicrol exerts antiangiogenic and antitumor effects in a mouse melanoma (B16f10) allograft model. *Evid Based Complement Alternat Med.* (2020) 2020:8543872. doi: 10.1155/2020/8543872
- Goenka S, Simon SR. Organogold drug auranofin exhibits anti-melanogenic activity in B16f10 and Mnt-1 melanoma cells. *Arch Dermatol Res.* (2020) 312:213–21. doi: 10.1007/s00403-019-01974-1
- Guo L, Kang JS, Kang NJ, Choi YWS-. Ptasin induces apoptosis and inhibits cell migration through activation of P53 pathway signaling in melanoma B16f10 Cells and A375 Cells. *Arch Biochem Biophys.* (2020) 692:108519. doi: 10.1016/j.abb.2020.108519
- Huang HC, Wang SS, Tsai TC, Ko WP, Chang TM. Phoenix Dactylifera L. Seed extract exhibits antioxidant effects and attenuates melanogenesis in B16f10 murine melanoma cells by downregulating Pka signaling. *Antioxidants.* (2020) 9:1270. doi: 10.3390/antiox9121270
- Nam G, An SK, Park IC, Bae S, Lee JH. Daphnetin inhibits alpha-Msh-induced melanogenesis via Pka and Erk signaling pathways in B16f10 melanoma cells. *Biosci Biotechnol Biochem.* (2022) 86:596–609. doi: 10.1093/bbb/zba c016
- Zhang L, Zhu L, Yao X, Lou X, Wan J, Duan X, et al. Paclitaxel treatment enhances lymphatic metastasis of B16f10 melanoma cells via Ccl21/Ccr7 Axis. *Int J Biol Sci.* (2022) 18:1476–90. doi: 10.7150/ijbs.67138
- Schomberg J, Wang Z, Farhat A, Guo KL, Xie J, Zhou Z, et al. Luteolin inhibits melanoma growth in vitro and in vivo via regulating Ecm and oncogenic pathways but not Ros. *Biochem Pharmacol.* (2020) 177:114025. doi: 10.1016/j.bcp.2020.114025
- Liu HM, Lei SN, Tang W, Xun MH, Zhao ZW, Cheng MY, et al. Optimization of ultrasound-assisted cellulase extraction from nymphaea hybrid flower and biological activities: antioxidant activity, protective effect against Ros oxidative damage in hacat cells and inhibition of melanin production in B16 cells. *Molecules.* (2022) 27:1914. doi: 10.3390/molecules27061914

NZ participated in manuscript writing. QC revised the manuscript. All authors contributed to the article and approved the submitted version.

Funding

This work was supported by the Zhejiang Provincial Top Discipline of Biological Engineering (Level A) (Grant number: KF2022004) and the Zhejiang Provincial Natural Science Foundation of China (LQ18C200001).

Conflict of interest

The authors declare that the research was conducted in the absence of any commercial or financial relationships that could be construed as a potential conflict of interest.

Publisher's note

All claims expressed in this article are solely those of the authors and do not necessarily represent those of their affiliated organizations, or those of the publisher, the editors and the reviewers. Any product that may be evaluated in this article, or claim that may be made by its manufacturer, is not guaranteed or endorsed by the publisher.

15. Chen S, Zhao X, Wan J, Ran L, Qin Y, Wang X, et al. Dihydromyricetin improves glucose and lipid metabolism and exerts anti-inflammatory effects in nonalcoholic fatty liver disease: a randomized controlled trial. *Pharmacol Res.* (2015) 99:74–81. doi: 10.1016/j.phrs.2015.05.009
16. Jiang B, Le L, Pan H, Hu K, Xu L, Xiao P. Dihydromyricetin ameliorates the oxidative stress response induced by methylglyoxal via the Ampk/Glut4 signaling pathway in Pc12 Cells. *Brain Res Bull.* (2014) 109:117–26. doi: 10.1016/j.brainresbull.2014.10.010
17. Ye L, Wang H, Duncan SE, Eigel WN, O'Keefe SF. Antioxidant activities of vine tea (*Ampelopsis Grossedentata*) extract and its major component dihydromyricetin in soybean oil and cooked ground beef. *Food Chem.* (2015) 172:416–22. doi: 10.1016/j.foodchem.2014.09.090
18. Xiao XN, Wang F, Yuan YT, Liu J, Liu YZ, Yi X. Antibacterial activity and mode of action of dihydromyricetin from *ampelopsis grossedentata* leaves against food-borne bacteria. *Molecules.* (2019) 24:2831. doi: 10.3390/molecules24152831
19. Hou XL, Tong Q, Wang WQ, Shi CY, Xiong W, Chen J, et al. Suppression of inflammatory responses by dihydromyricetin, a flavonoid from *ampelopsis grossedentata*, via inhibiting the activation of Nf-Kappab and mapk signaling pathways. *J Nat Prod.* (2015) 78:1689–96. doi: 10.1021/acs.jnatprod.5b00275
20. Wu J, Zhao FT, Fan KJ, Zhang J, Xu BX, Wang QS, et al. Dihydromyricetin inhibits inflammation of fibroblast-like synoviocytes through regulation of nuclear factor-kappab signaling in rats with collagen-induced arthritis. *J Pharmacol Exp Ther.* (2019) 368:218–28. doi: 10.1124/jpet.118.253369
21. Zhang Q, Zhao Y, Zhang M, Zhang Y, Ji H, Shen L. Recent advances in research on vine tea, a potential and functional herbal tea with dihydromyricetin and myricetin as major bioactive compounds. *J Pharm Anal.* (2021) 11:555–63. doi: 10.1016/j.jpha.2020.10.002
22. Zhu L, Zhang B, Luo J, Dong S, Zang K, Wu Y. Ampelopsin-sodium induces apoptosis in human lung adenocarcinoma cell lines by promoting tubulin polymerization in vitro. *Oncol Lett.* (2019) 18:189–96. doi: 10.3892/ol.2019.10288
23. Guo Z, Guozhang H, Wang H, Li Z, Liu N. Ampelopsin inhibits human glioma through inducing apoptosis and autophagy dependent on ros generation and Jnk pathway. *Biomed Pharmacother.* (2019) 116:108524. doi: 10.1016/j.biopha.2018.12.136
24. Li X, Yang ZS, Cai WW, Deng Y, Chen L, Tan SL. Dihydromyricetin inhibits tumor growth and epithelial-mesenchymal transition through regulating Mir-455-3p in cholangiocarcinoma. *J Cancer.* (2021) 12:6058–70. doi: 10.7150/jca.61311
25. Dong Y, Zhao Q, Wang Y. Network pharmacology-based investigation of potential targets of astragalus membranaceus-angelica sinensis compound acting on diabetic nephropathy. *Sci Rep.* (2021) 11:19496. doi: 10.1038/s41598-021-98925-6
26. Baust JM, Buehring GC, Campbell L, Elmore E, Harbell JW, Nims RW, et al. Best practices in cell culture: an overview. *Vitro Cell Dev Biol Anim.* (2017) 53:669–72. doi: 10.1007/s11626-017-0177-7
27. Nordin NA, Lawai V, Ngaini Z, Abd Halim AN, Hwang SS, Linton RE, et al. *In vitro* cytotoxicity evaluation of thiourea derivatives bearing *Salix* sp. constituent against Hk-1 cell lines. *Nat Prod Res.* (2020) 34:1505–14. doi: 10.1080/14786419.2018.1517120
28. Chou TC, Talalay P. Generalized equations for the analysis of inhibitions of michaelis-menten and higher-order kinetic systems with two or more mutually exclusive and nonexclusive inhibitors. *Eur J Chem.* (1981) 115:207–16.
29. Crowley LC, Marfell BJ, Waterhouse NJ. Analyzing cell death by nuclear staining with hoechst 33342. *Cold Spring Harb. Protoc.* (2016) 2016:778–81. doi: 10.1101/pdb.prot087205
30. Jenson EC. Quantitative analysis of histological staining and fluorescence using imagej. *Anat Rec.* (2013) 296:378–81.
31. Promden W, Viriyabancha W, Monthakantirat O, Umehara K, Noguchi H, De-Eknamkul W. Correlation between the potency of flavonoids on mushroom tyrosinase inhibitory activity and melanin synthesis in melanocytes. *Molecules.* (2018) 23:1403. doi: 10.3390/molecules23061403
32. Krupnick ASKD, Szeto WY, Popma SH, Amin KM, Moore JS, Rosengard BR. Multiparameter flow cytometric approach for simultaneous evaluation of T lymphocyte-endothelial cell interactions. *Cytometry.* (2001) 46:271–80. doi: 10.1002/cyto.1168
33. Choi EO, Lee H, HwangBo H, Kwon DH, Kim MY, Ji SY, et al. Citrus unshiu peel suppress the metastatic potential of murine melanoma b16f10 cells in vitro and in vivo. *Phytother Res.* (2019) 33:3228–41. doi: 10.1002/ptr.6497
34. Han Y, Li X, Yan J, Ma C, Wang X, Pan H, et al. Bioinformatic analysis identifies potential key genes in the pathogenesis of melanoma. *Front. Oncol.* (2020) 10:581985. doi: 10.3389/fonc.2020.581985
35. Uscanga-Palomeque AC, Zapata-Benavides P, Saavedra-Alonso S, Zamora-Avila DE, Franco-Molina MA, Arellano-Rodriguez M, et al. Inhibitory effect of *cuphea aequipetala* extracts on murine B16f10 melanoma in vitro and in vivo. *Biomed Res Int.* (2019) 2019:8560527. doi: 10.1155/2019/8560527
36. Menke K, Schwermer M, Felenda J, Beckmann C, Stintzing F, Schramm A, et al. Taraxacum officinale extract shows antitumor effects on pediatric cancer cells and enhance mistletoe therapy. *Complement Ther Med.* (2018) 40:158–64. doi: 10.1016/j.ctim.2018.03.005
37. Sturza A, Pavel I, Ancusa S, Danciu C, Dehelean C, Duicu O, et al. Quercetin exerts an inhibitory effect on cellular bioenergetics of the B164a5 murine melanoma cell line. *Mol Cell Biochem.* (2018) 447:103–9. doi: 10.1007/s11010-018-3296-x
38. Ponte LGS, Pavan ICB, Mancini MCS, da Silva LGS, Morelli AP, Severino MB, et al. The hallmarks of flavonoids in cancer. *Molecules.* (2021) 26:2029. doi: 10.3390/molecules26072029
39. Huang HC, Liao CC, Peng CC, Lim JM, Siao JH, Wei CM, et al. Dihydromyricetin from *ampelopsis grossedentata* inhibits melanogenesis through down-regulation of Mapk, Pka and Pkc signaling pathways. *Chem Biol Interact.* (2016) 258:166–74. doi: 10.1016/j.cbi.2016.08.023
40. Itoh KHN, Masuda M, Naruto S, Murata K, Wakabayashi K, Matsuda H. Inhibitory effects of citrus hassaku extract and its flavanone glycosides on melanogenesis. *Biol Pharm Bull.* (2009) 32:410–5. doi: 10.1248/bpb.32.410
41. Kubo I, Kinoshita Hori I. Flavonols from saffron flower: tyrosinase inhibitory activity and inhibition mechanism. *J Agric Food Chem.* (1999) 47:4121–5. doi: 10.1021/jf990201q
42. Caesar LK, Cech NB. Synergy and antagonism in natural product extracts: when 1 + 1 does not equal 2. *Nat Prod Rep.* (2019) 36:869–88. doi: 10.1039/c9np00011a
43. Nöldner M, Schötz K. Rutin is essential for the antidepressant activity of hypericum perforatum extracts in the forced swimming test. *Planta Med.* (2002) 68:577–80. doi: 10.1055/s-2002-32908
44. Xu A, Lee J, Zhao Y, Wang Y, Li X, Xu P. Potential effect of Egcg on the anti-tumor efficacy of metformin in melanoma cells. *J Zhejiang Univ Sci B.* (2021) 22:548–62. doi: 10.1631/jzus.B2000455
45. Fang Y, DeMarco VG, Nicholl MB. Resveratrol enhances radiation sensitivity in prostate cancer by inhibiting cell proliferation and promoting cell senescence and apoptosis. *Cancer Sci.* (2012) 103:1090–8. doi: 10.1111/j.1349-7006.2012.02272.x
46. Tang SM, Deng XT, Zhou J, Li QP, Ge XX, Miao L. Pharmacological basis and new insights of quercetin action in respect to its anti-cancer effects. *Biomed Pharmacother.* (2020) 121:109604. doi: 10.1016/j.biopha.2019.109604
47. Harris Z, Donovan MG, Branco GM, Limesand KH, Burd R. Quercetin as an emerging anti-melanoma agent: a four-focus area therapeutic development strategy. *Front Nutr.* (2016) 3:48. doi: 10.3389/fnut.2016.00048
48. Davenport A, Frezza M, Shen M, Ge Y, Huo C, Chan TH, et al. Celastrol and an Egcg pro-drug exhibit potent chemosensitizing activity in human leukemia cells. *Int J Mol Med.* (2010) 25:465–70. doi: 10.3892/ijmm.00000366
49. Ji X, Wei X, Qian J, Mo X, Kai G, An F, et al. 2',4'-Dihydroxy-6'-Methoxy-3',5'-dimethylchalcone induced apoptosis and G1 cell cycle arrest through Pi3k/Akt pathway in bel-7402/5-Fu Cells. *Food Chem Toxicol.* (2019) 131:110533. doi: 10.1016/j.fct.2019.05.041
50. Lu R, Serrero G. Resveratrol, a natural product derived from grape, exhibits antiestrogenic activity and inhibits the growth of human breast cancer cells. *J Cell Physiol.* (1999) 179:297–304. doi: 10.1002/(SICI)1097-4652(199906)179:3<297::AID-JCP78>3.0.CO;2-P
51. Kai W, Yating S, Lin M, Kaiyong Y, Baojin H, Wu Y, et al. Natural product toosendanin reverses the resistance of human breast cancer cells to adriamycin as a novel Pi3k inhibitor. *Biochem Pharmacol.* (2018) 152:153–64. doi: 10.1016/j.bcp.2018.03.022
52. Kanapathipillai M. Treating P53 mutant aggregation-associated cancer. *Cancers.* (2018) 10:154. doi: 10.3390/cancers10060154
53. Prasad S, Ravindran J, Aggarwal BB. Nf-Kappab and cancer: how intimate is this relationship. *Mol Cell Biochem.* (2010) 336:25–37. doi: 10.1007/s11010-009-0267-2
54. Sample A, He YY. Mechanisms and prevention of Uv-induced melanoma. *Photodermatol Photoimmunol Photomed.* (2018) 34:13–24. doi: 10.1111/phpp.12329
55. Tian X, Cui Z, Liu S, Zhou J, Cui R. Melanosome transport and regulation in development and disease. *Pharmacol Ther.* (2021) 219:107707. doi: 10.1016/j.pharmthera.2020.107707
56. Melnikova VO, Balasubramanian K, Villares GJ, Dobroff AS, Zigler M, Wang H, et al. Crosstalk between protease-activated receptor 1 and platelet-activating factor receptor regulates melanoma cell adhesion molecule (Mcam/Muc18) expression and melanoma metastasis. *J Biol Chem.* (2009) 284:28845–55. doi: 10.1074/jbc.M109.042150